Electronic Supplementary Material (ESI) for Journal of Materials Chemistry A.

Supporting Information

Changes of coordination modes of Cu-based coordination polymers as tuneable proton-conducting solid electrolytes

Mei-Jie Wei, Jia-Qi Fu, Yi-Di Wang, Jing-Yang Gu, Bai-Ling Liu, Hong-Ying Zang*, En-Long Zhou, Kui-Zhan Shao, Zhong-Min Su*

Institute of Functional Material Chemistry, Key Lab of Polyoxometalate, Science of Ministry of Education, Faculty of Chemistry, Northeast Normal University, Changchun, 130024, Jilin, People's Republic of China.E-mail: zanghy100@nenu.edu.cn; zmsu@nenu.edu.cn Fax: +860431-85684009; Tel: +860431-85099108

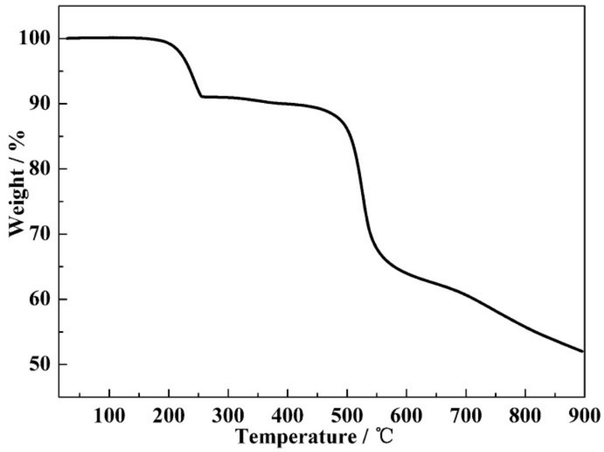

Fig. S1 TGA curve of compound **1**.

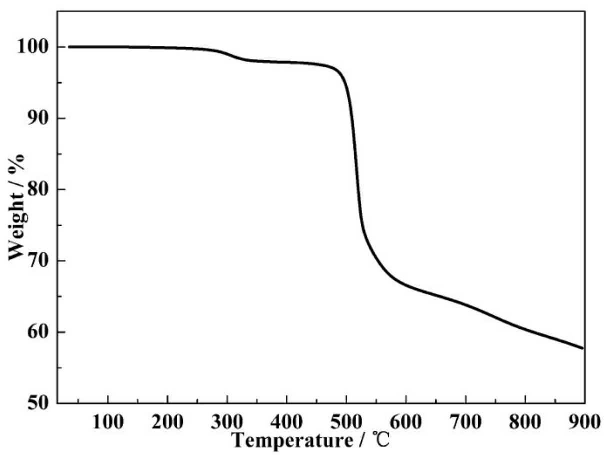

Fig. S2 TGA curve of compound **2**.

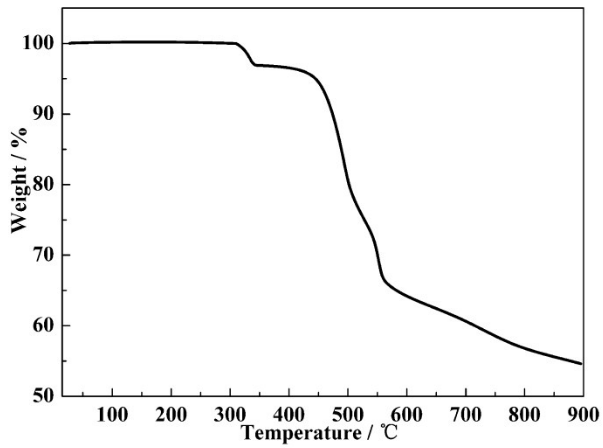

Fig. S3 TGA curve of compound **3**.

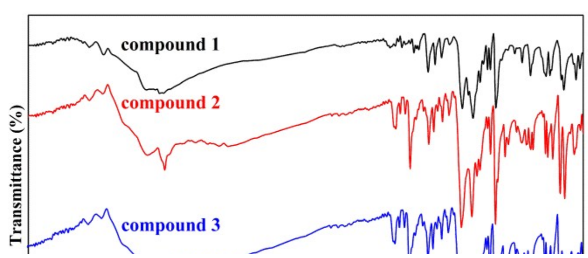

Fig. S4 FT-IR spectra of compounds.

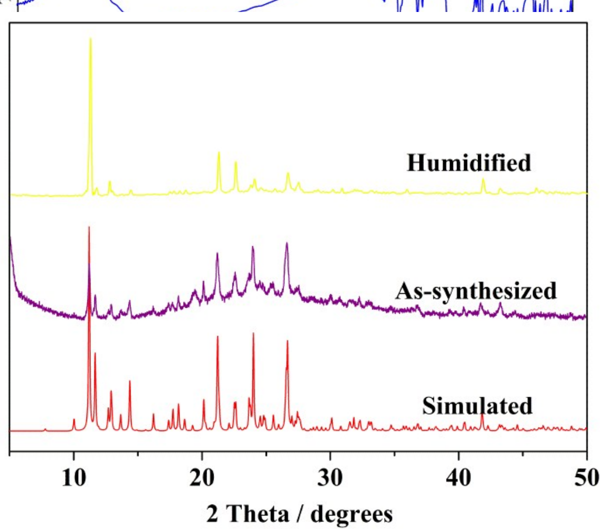

Fig. S5 PXRD patterns of compound **1**; simulated pattern (bottorn trace), as-synthesized pattern (middle), and for a sample that was treated after impedance measurement at 95 °C and 97% RH (top).

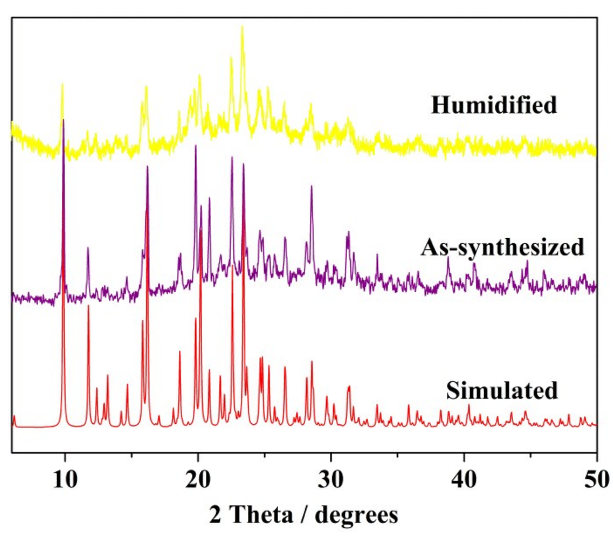

Fig. S6 PXRD patterns of compound **2**; simulated pattern (bottorn trace), as-synthesized pattern (middle), and for a sample that was treated after impedance measurement at 95 °C and 97% RH (top).

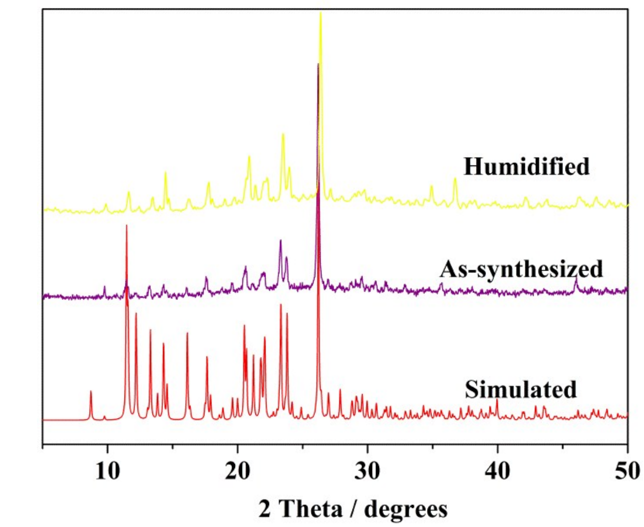

Fig. S7 PXRD patterns of compound **3**; simulated pattern (bottorn trace), as-synthesized pattern (middle), and for a sample that was treated after impedance measurement at 95 °C and 97% RH (top).

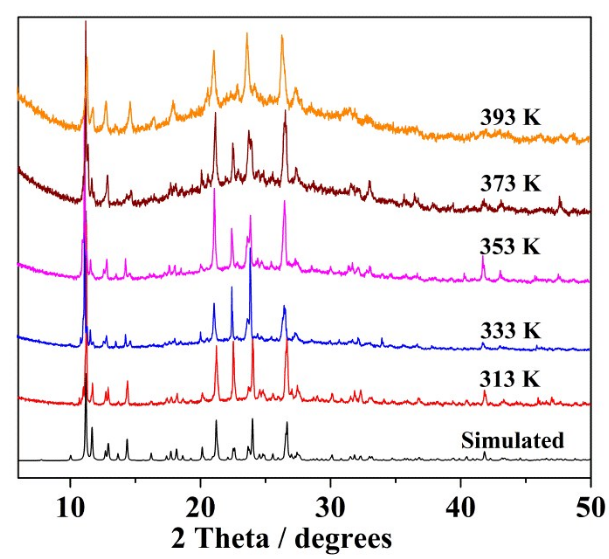

Fig. S8 Simulated and variable-temperature PXRD patterns of compound **1**.

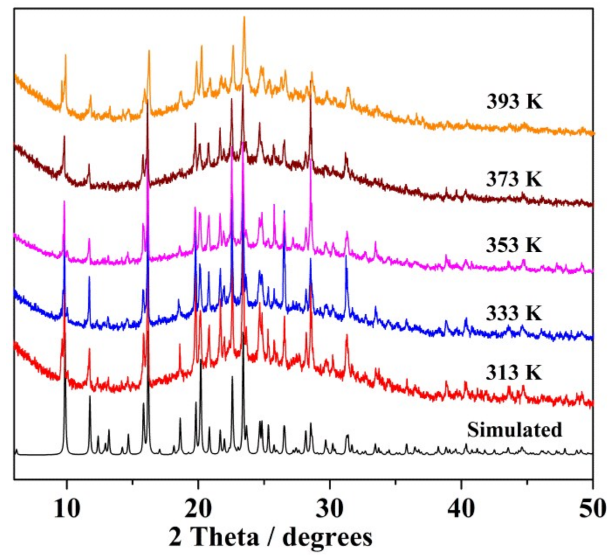

Fig. S9 Simulated and variable-temperature PXRD patterns of compound **2**.

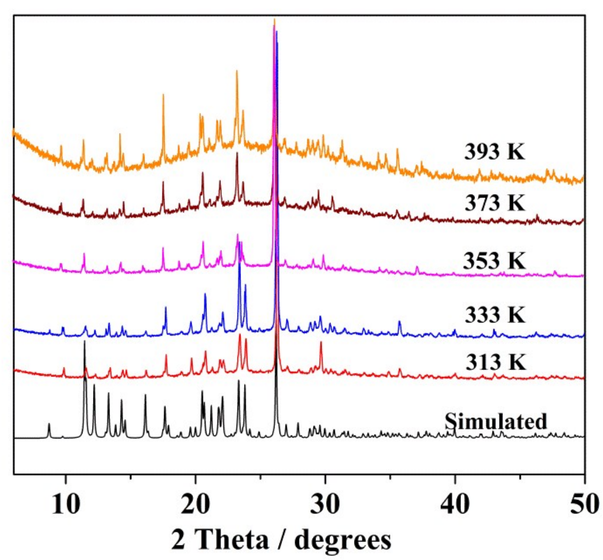

Fig. S10 Simulated and variable-temperature PXRD patterns of compound **3**.

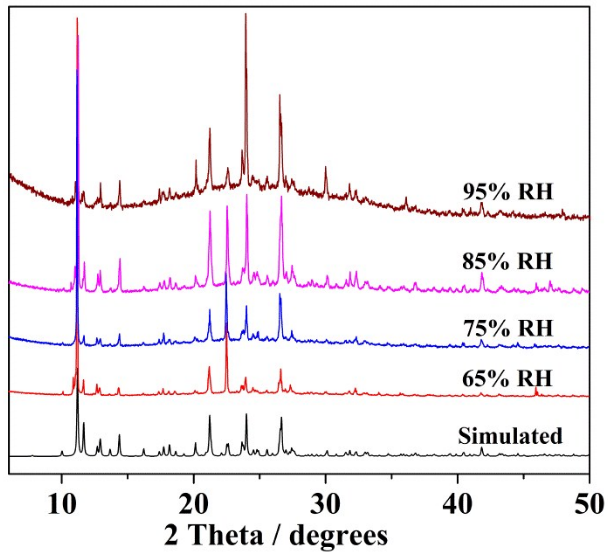

Fig. S11 Simulated and variable-humidity PXRD patterns of compound **1** at 25 °C and 65% RH, 75% RH, 85%RH and 95%RH.

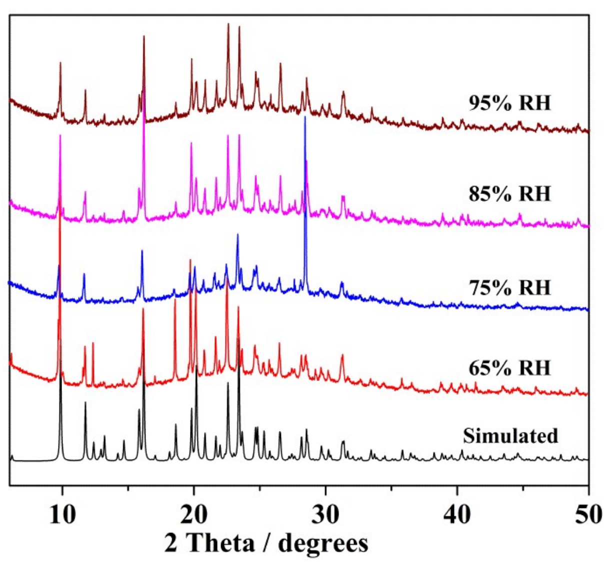

Fig. S12 Simulated and variable-humidity PXRD patterns of compound **2** at 25 °C and 65% RH, 75% RH, 85%RH and 95%RH.

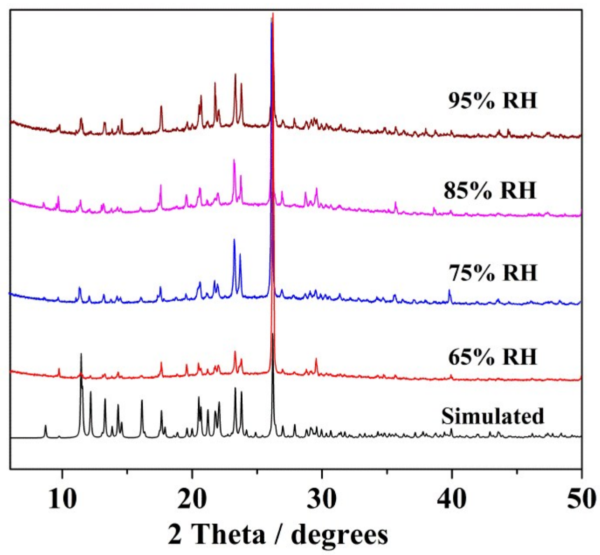

Fig. S13 Simulated and variable-humidity PXRD patterns of compound **3** at 25 °C and 65% RH, 75% RH, 85%RH and 95%RH.

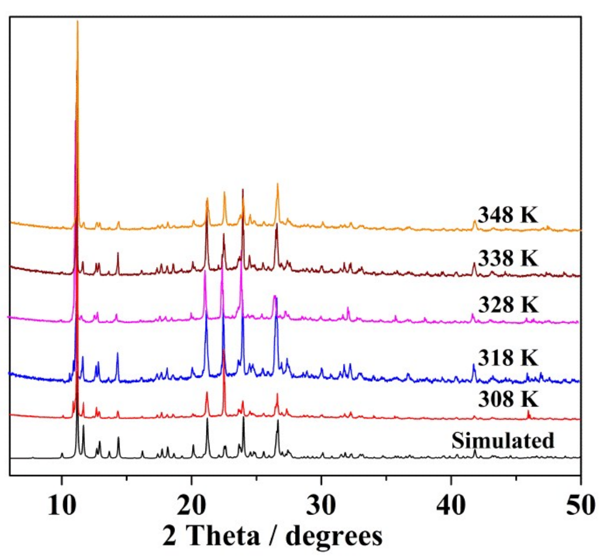

Fig. S14 PXRD patterns of compound **1**; simulated pattern, and for samples that was treated at 85% RH and corresponding temperature after impedance measurement.

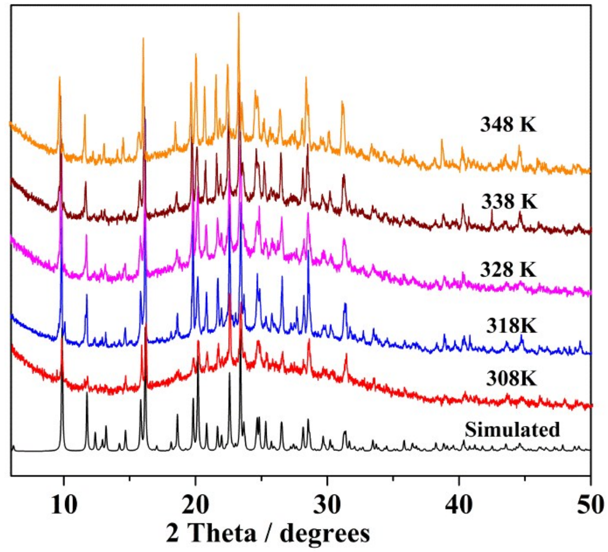

Fig. S15 PXRD patterns of compound **2**; simulated pattern, and for samples that was treated at 85% RH and corresponding temperature after impedance measurement.

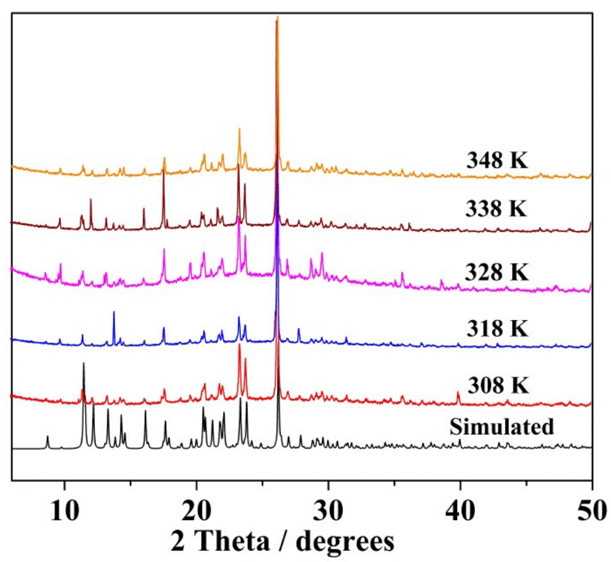

Fig. S16 PXRD patterns of compound **3**; simulated pattern, and for samples that was treated at 85%

RH and corresponding temperature after impedance measurement.

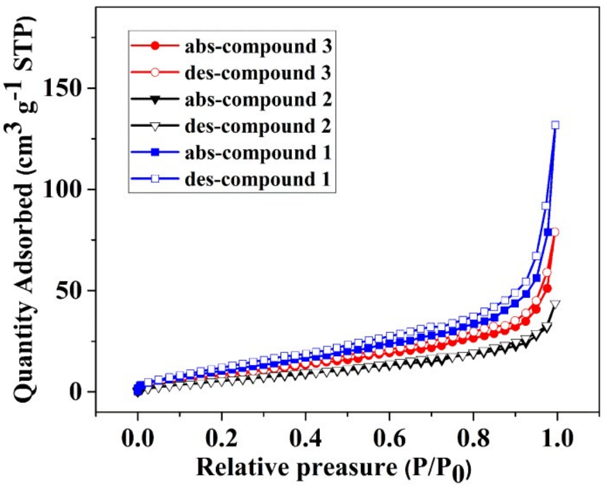

Fig. S17 N_2 adsorption isotherms for three compounds at 77 K.

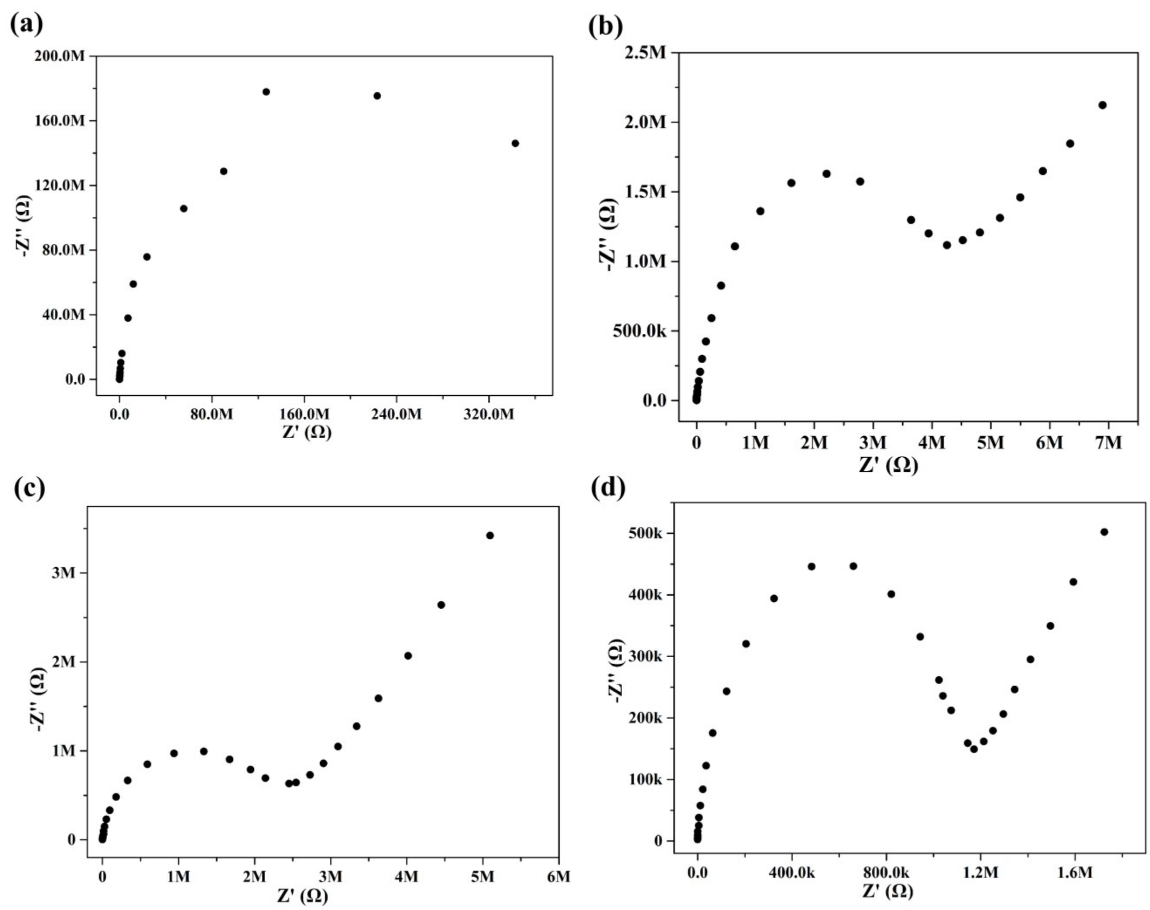

Fig. S18 Nyquist plot of compound **1** at 25 °C and 65% RH (a), 75% RH (b), 85% RH (c) and 95% RH (d) for first cycle.

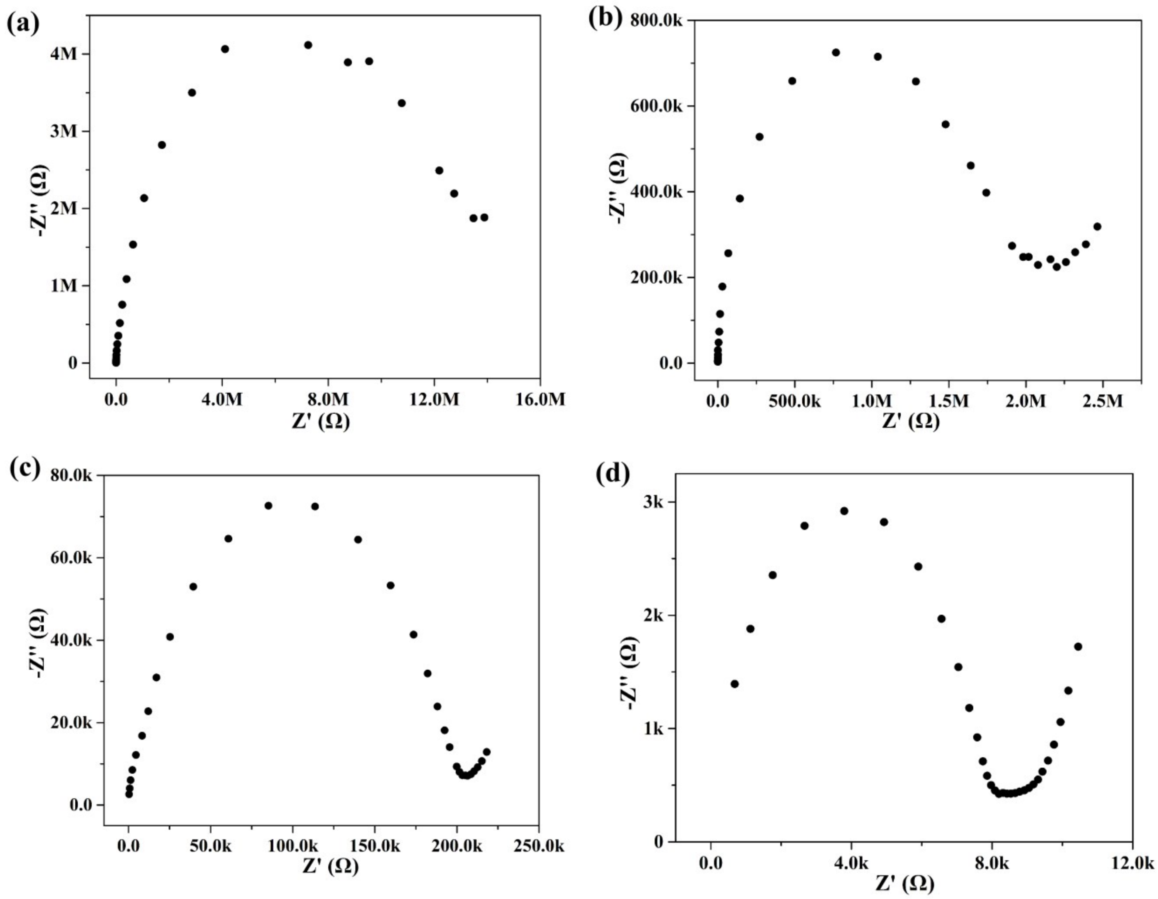

Fig. S19 Nyquist plot of compound **2** at 25 °C and 65% RH (a), 75% RH (b), 85% RH (c) and 95% RH (d) for first cycle.

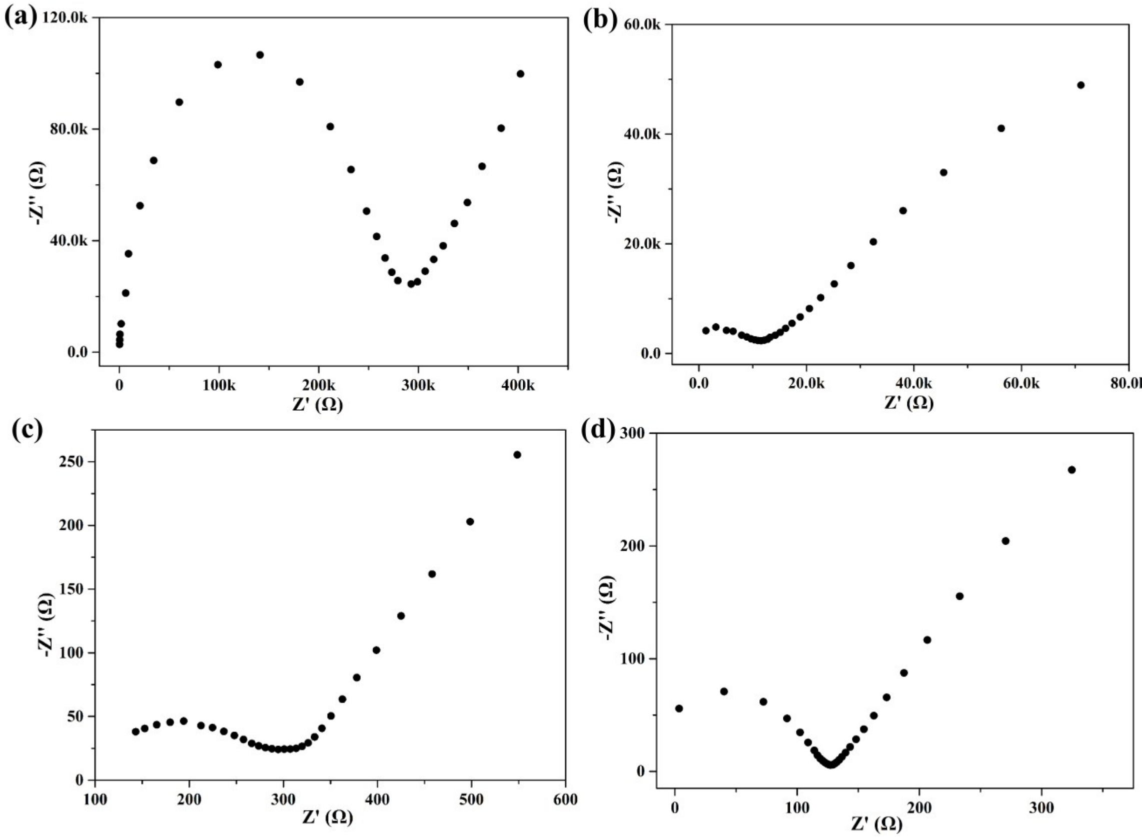

Fig. S20 Nyquist plot of compound **3** at 25 °C and 65% RH (a), 75% RH (b), 85% RH (c) and 95% RH (d) for first cycle.

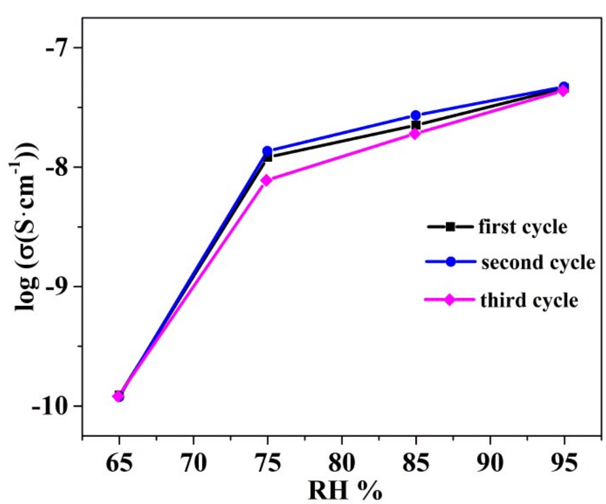

Fig. S21 The variable-humidity reproducibility of the proton conduction data of compound **1** for three cycles of measurement.

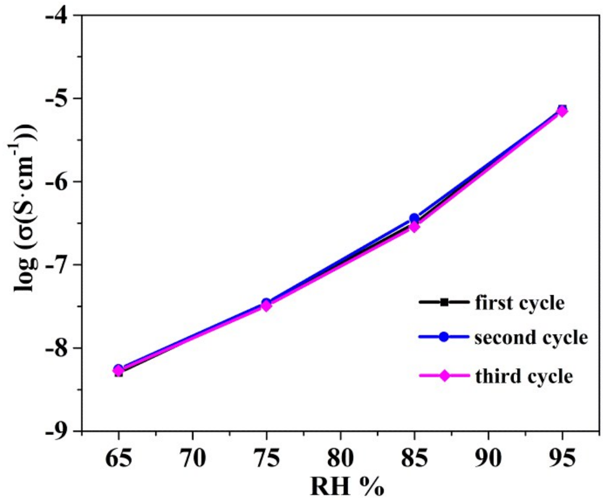

Fig. S22 The variable-humidity reproducibility of the proton conduction data of compound **2** for three cycles of measurement.

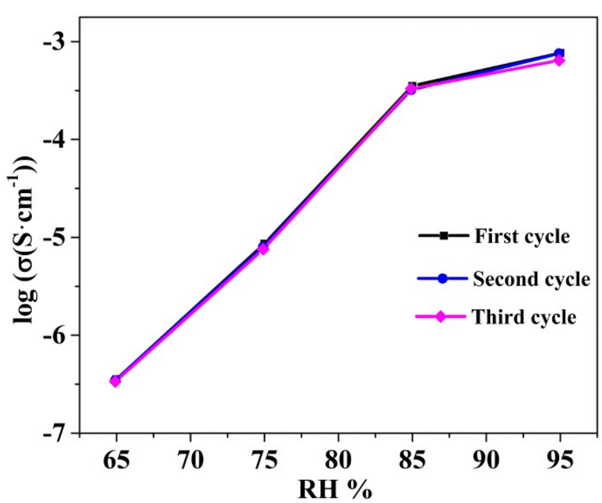

Fig. S23 The variable-humidity reproducibility of the proton conduction data of compound **3** for three cycles of measurement.

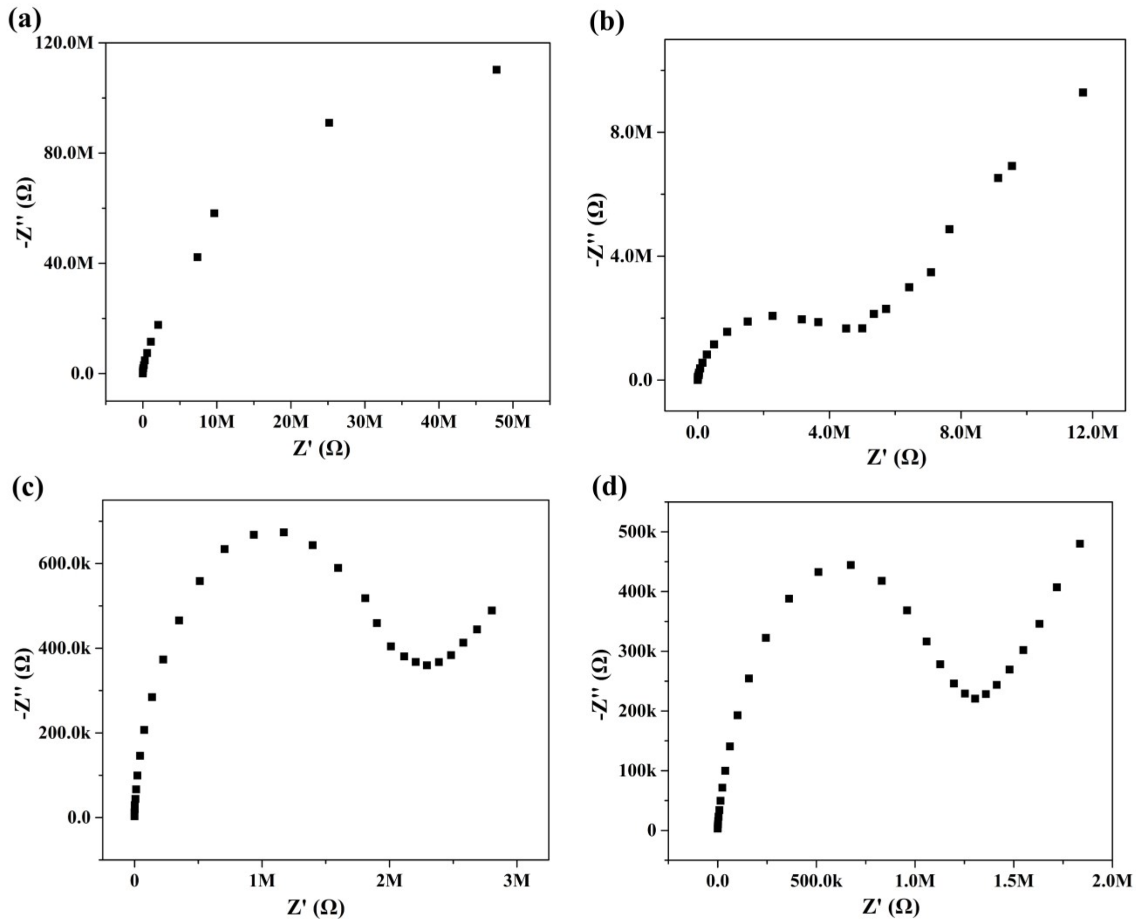

Fig. S24 The reproducibility of Nyquist plot of compound **1** at 25 °C and 65% RH (a), 75% RH (b), 85% RH (c) and 95% RH (d) for second cycle.

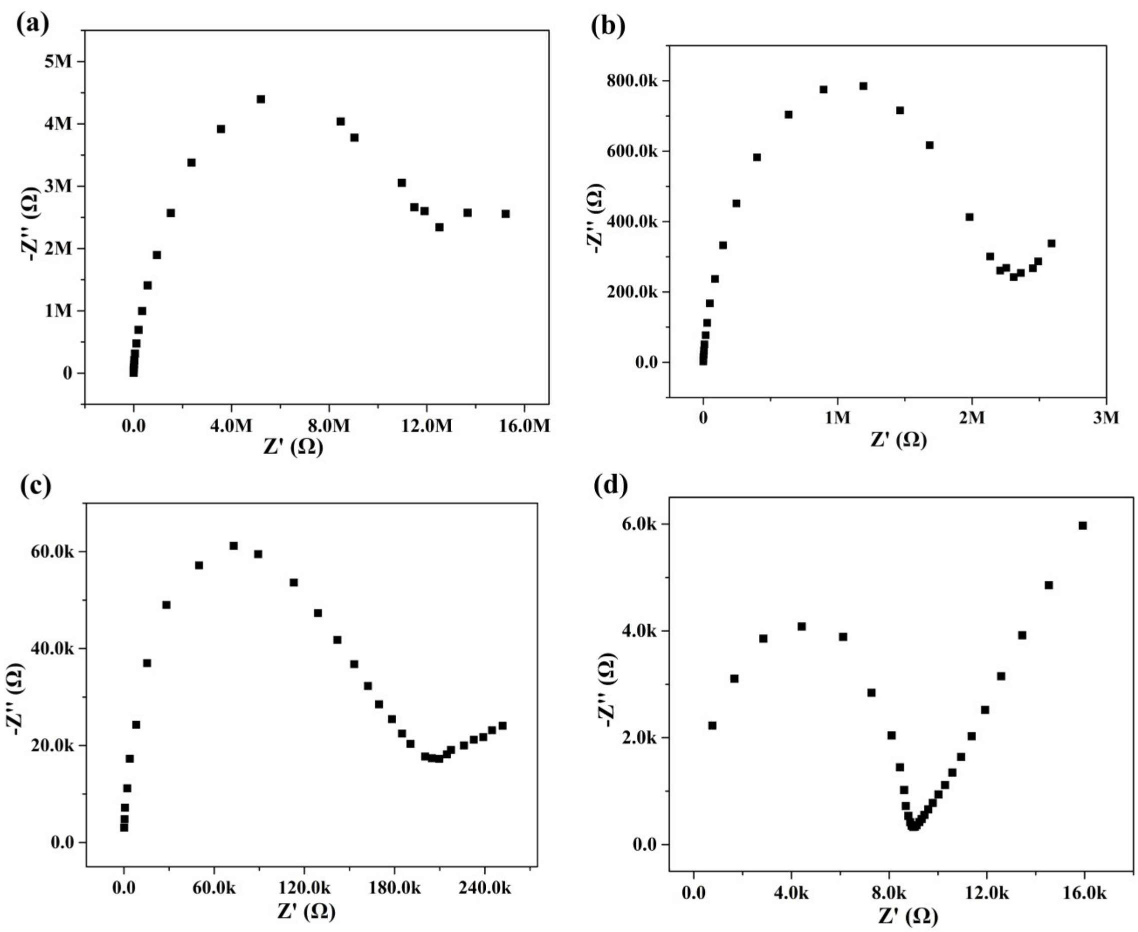

Fig. S25 The reproducibility of Nyquist plot of compound **2** at 25 °C and 65% RH (a), 75% RH (b), 85% RH (c) and 95% RH (d) for second cycle.

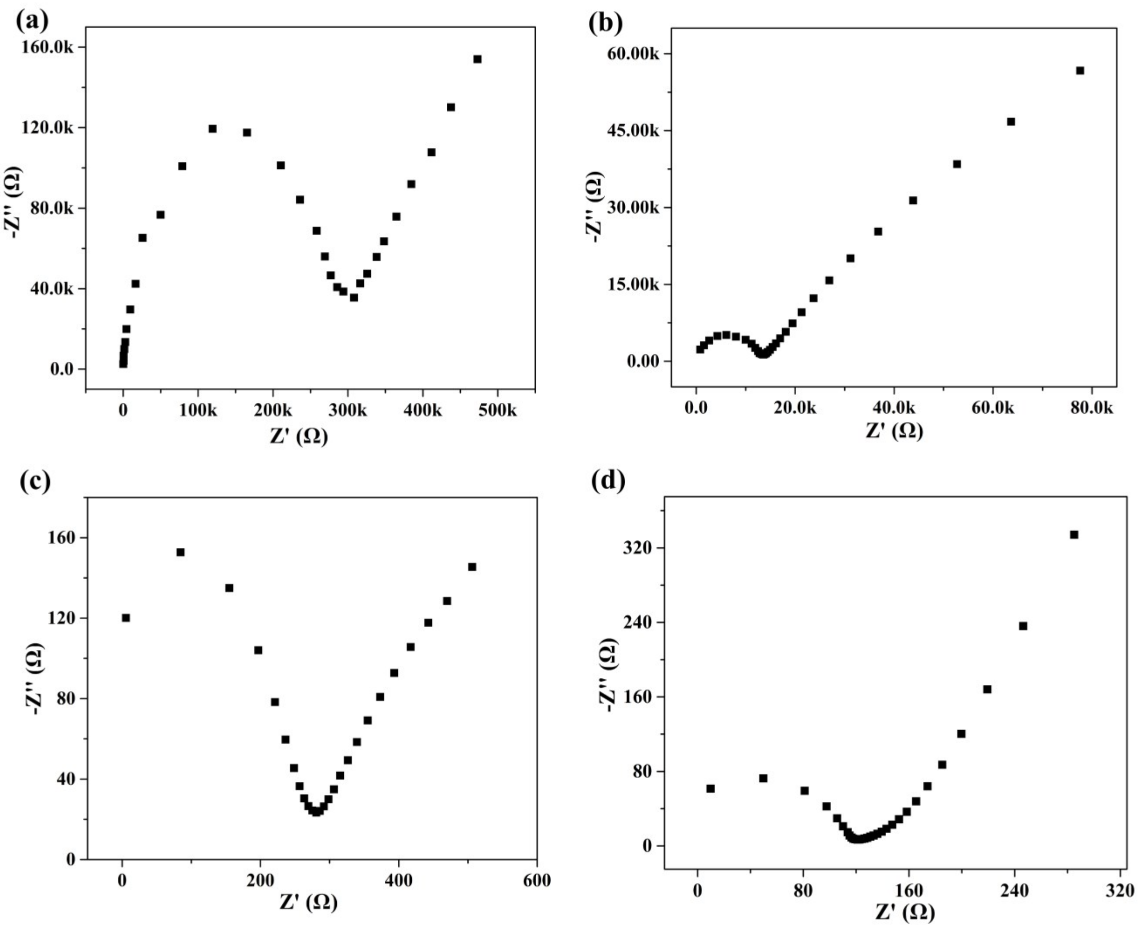

Fig. S26 The reproducibility of Nyquist plot of compound **3** at 25 °C and 65% RH (a), 75% RH (b), 85% RH (c) and 95% RH (d) for second cycle.

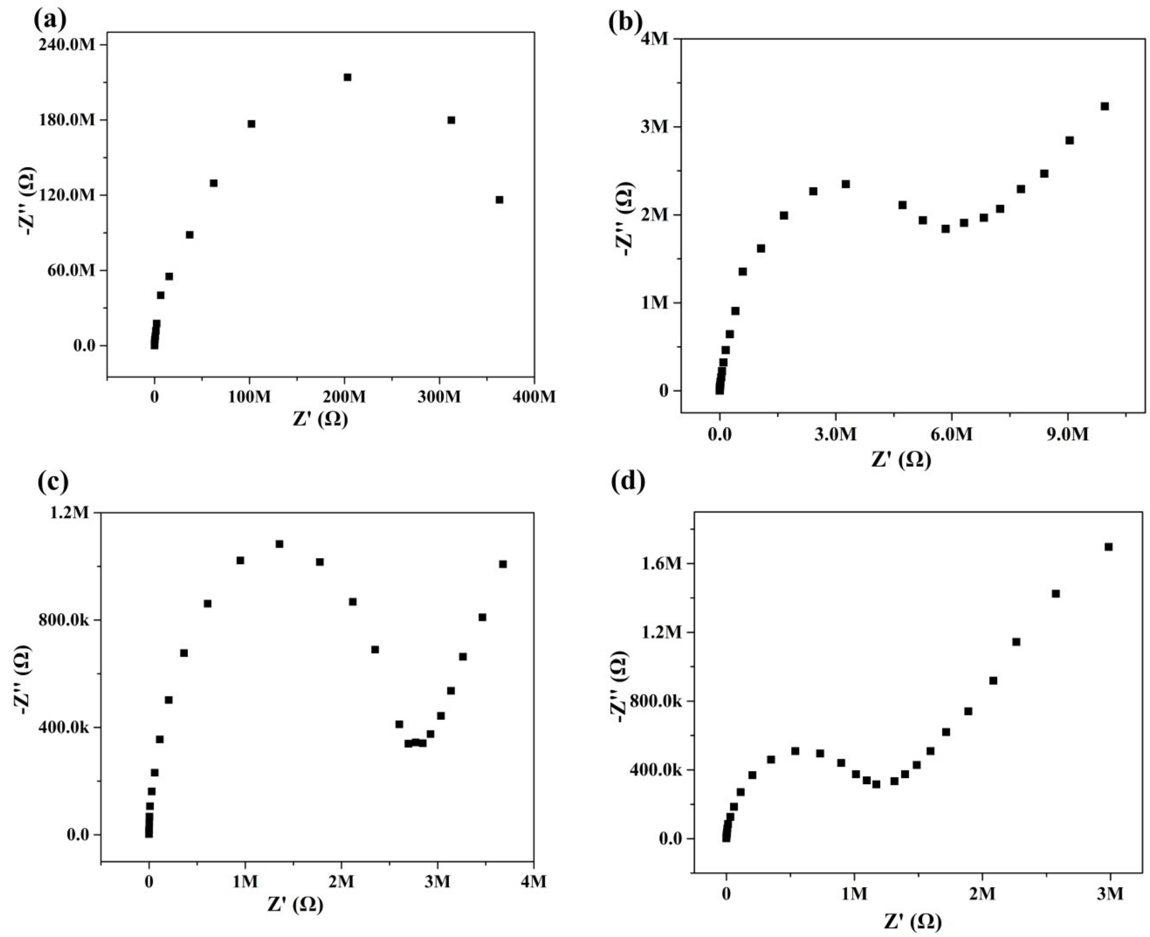

Fig. S27 The reproducibility of Nyquist plot of compound **1** at 25 °C and 65% RH (a), 75% RH (b), 85% RH (c) and 95% RH (d) for third cycle.

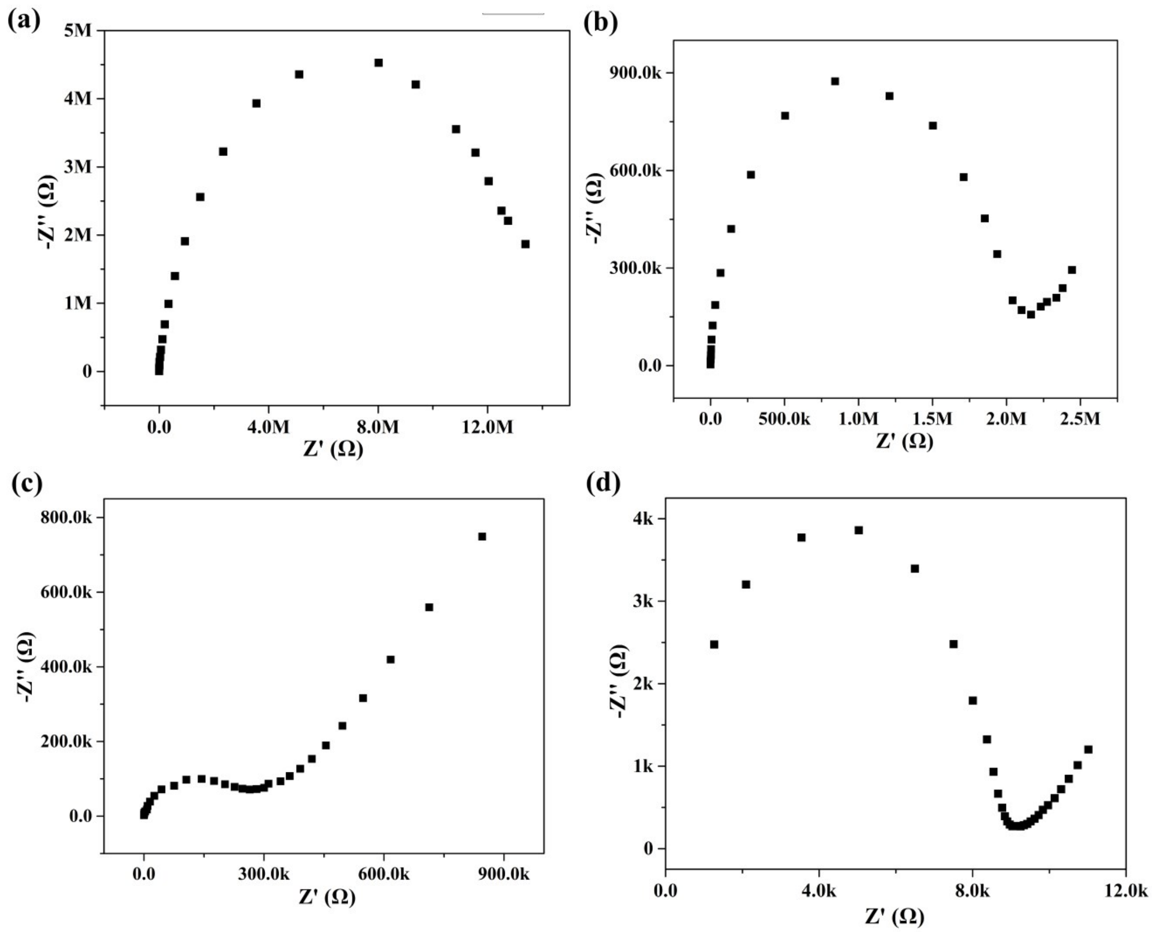

Fig. S28 The reproducibility of Nyquist plot of compound **2** at 25 °C and 65% RH (a), 75% RH (b), 85% RH (c) and 95% RH (d) for third cycle.

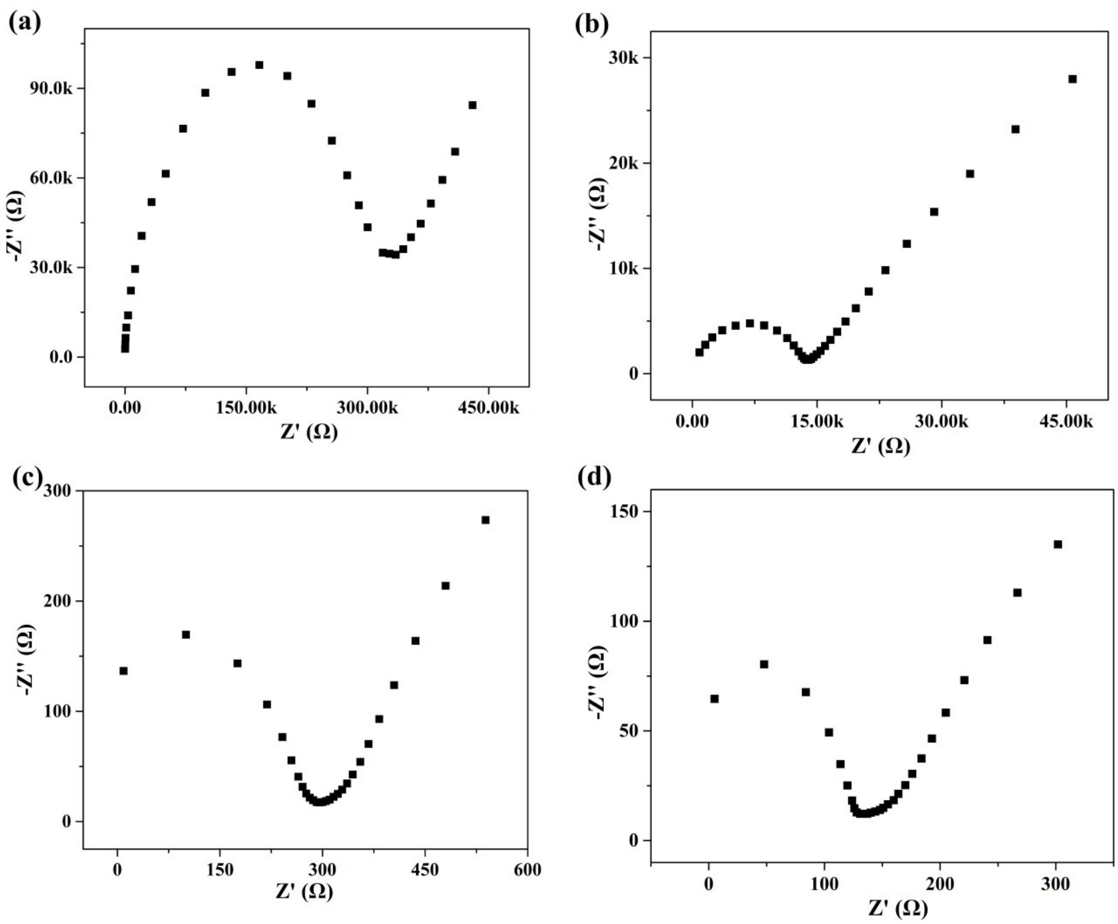

Fig. S29 The reproducibility of Nyquist plot of compound **3** at 25 °C and 65% RH (a), 75% RH (b), 85% RH (c) and 95% RH (d) for third cycle.

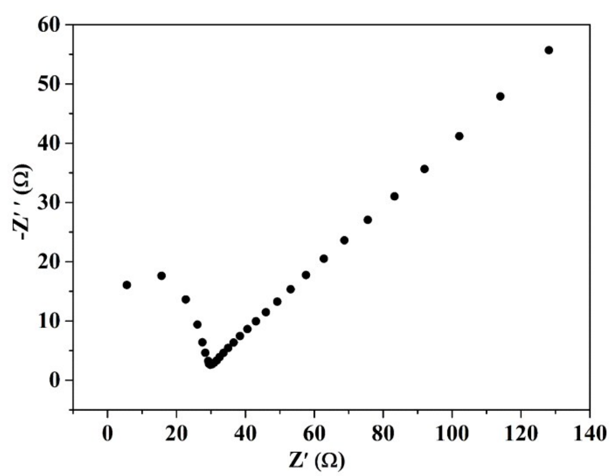

Fig. S30 Nyquist plot of compound **1** at 95 °C under 97% RH.

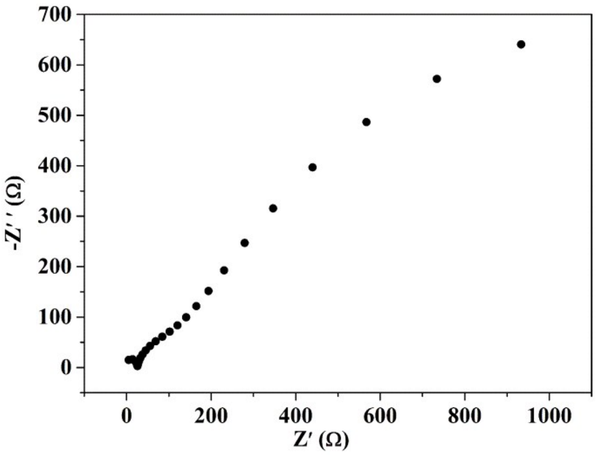

Fig. S31 Nyquist plot of compound **2** at 95 °C under 97% RH.

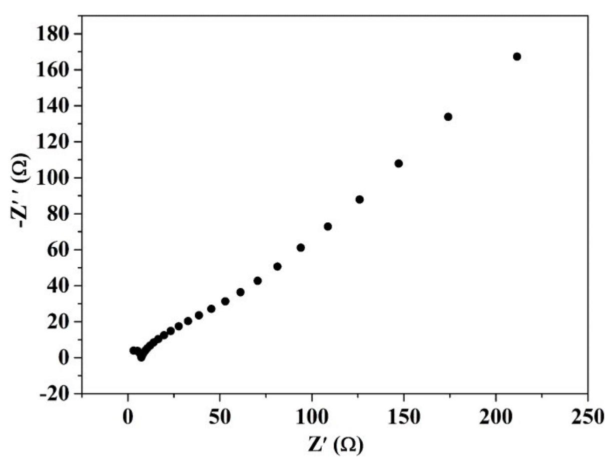

Fig. S32 Nyquist plot of compound **3** at 95 °C under 97% RH.

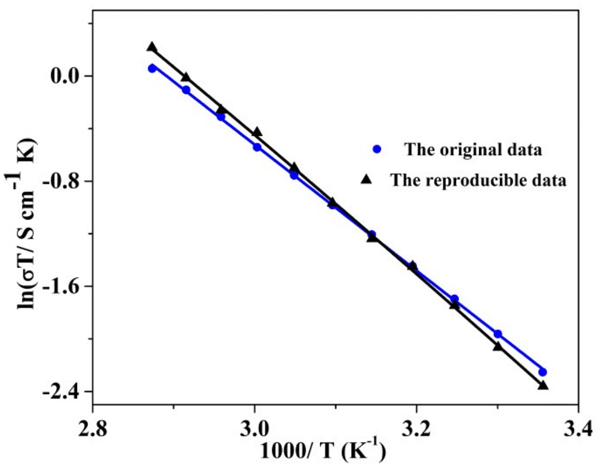

Fig. S33 The reproducibility of Arrhenius plots of the proton conductivity of compound **3** from 25 to 75 °C at 85% RH.

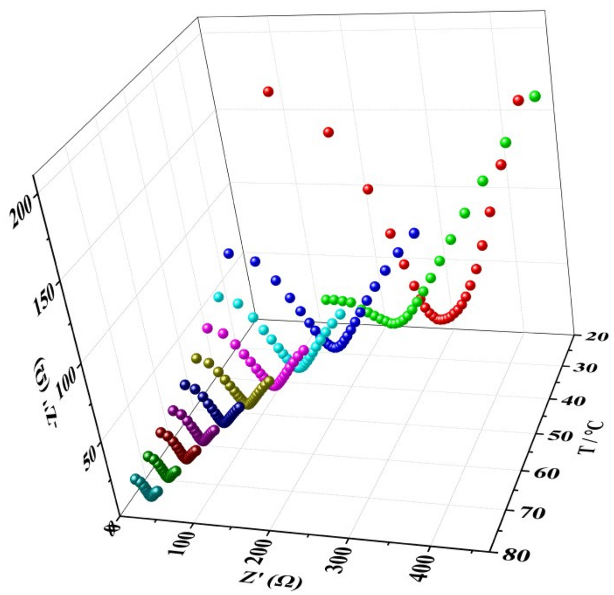

Fig. S34 The reproducibility of Nyquist plots of compound **3** at 85% RH and different temperatures of 25, 30, 35, 40, 45, 50, 55, 60, 65, 70 and 75 °C.

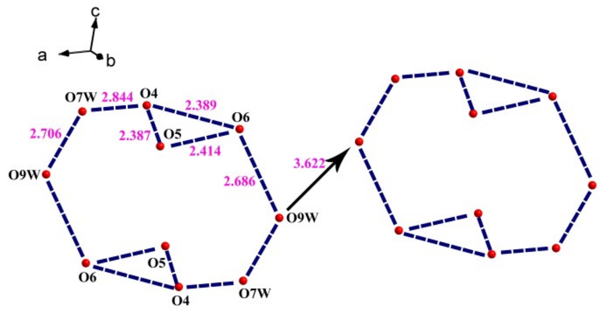

Fig. S35 Representation of hydrogen-bond network of compound **1**.

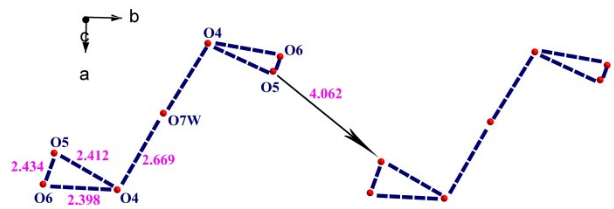

Fig. S36 Representation of hydrogen-bond network of compound **2**.

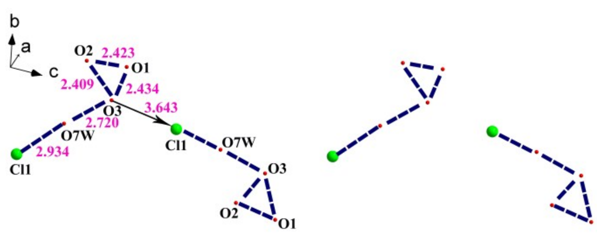

Fig. S37 Representation of hydrogen-bond network of compound **3**.

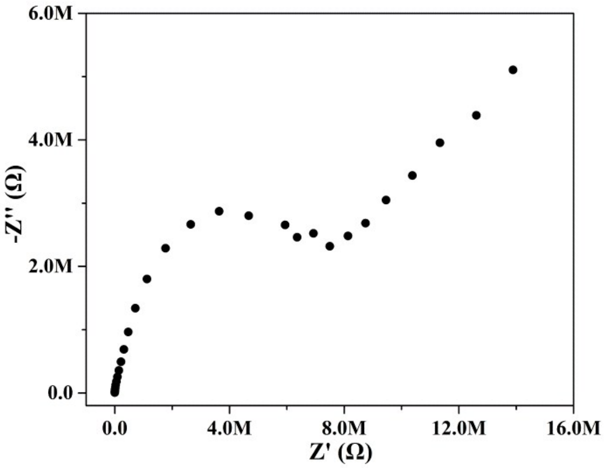

Fig. S38 Nyquist plot of compound **1** in presence of D_2O at 25 °C under 75% RH.

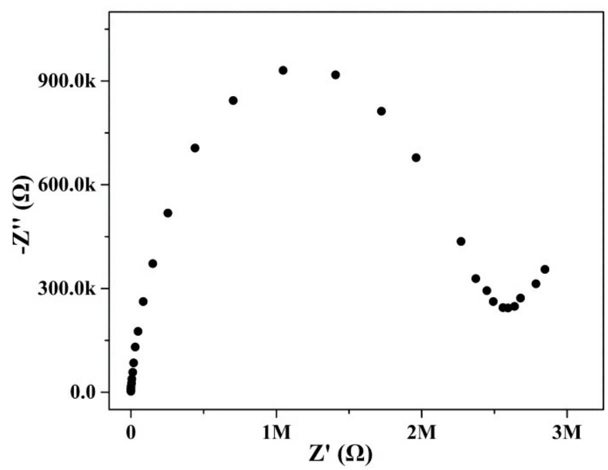

Fig. S39 Nyquist plot of compound **2** in presence of D_2O at 25 °C under 75% RH.

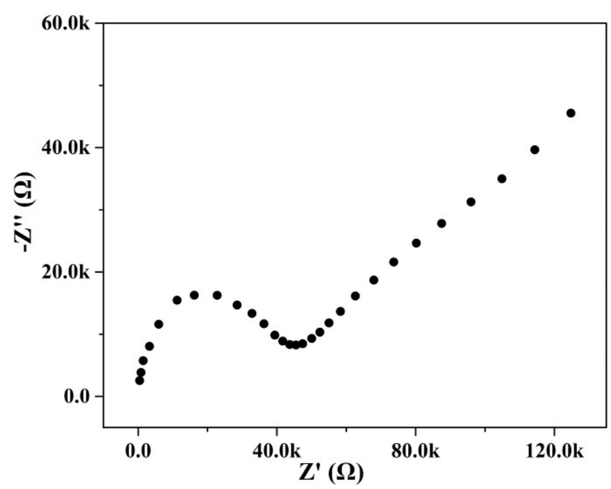

Fig. S40 Nyquist plot of compound **3** in presence of D_2O at 25 °C under 75% RH.

Table. S1 Crystal data and structure refinements for compound **1**、compound **2** and compound **3**.

Compound reference	**1**	**2**	**3**
Chemical formula	$C_{38}H_{32}N_8O_{18}S_4Cu_2$	$C_{38}H_{24}N_8O_{13}S_4Cu$	$C_{19}H_{13}N_4O_7S_2CuCl$
Formula Mass	1144.03	992.43	572.44
Crystal system	monoclinic	orthorhombic	monoclinic
a/(Å)	8.018(5)	28.561(5)	9.688(5)
b/(Å)	14.816(5)	9.430(5)	13.529(5)
c/(Å)	17.908(5)	13.827(5)	15.760(5)
α/°	90.000(5)	90.000(5)	90.000(5)
β/°	100.175(5)	90.000(5)	104.136(5)
γ/°	90.000(5)	90.000(5)	90.000(5)
Unit cell volume/(Å)$_3$	2093.9(16)	3724(2)	2003.1(14)
Temperature/K	293(2)	293(2)	293(2)
Space group	P 21/c	P c c n	P 21/n
No. of formula units per unit cell, Z	2	4	4
No. of reflections measured	4492	4702	3557
No. of independent reflections	3176	3893	2797
R_{int}	0.052	0.040	0.040
Final R_1 values (I> 2σ(I))^a	0.0411	0.0374	0.0340
Final $wR(F_2)$ values (I> 2σ(I))^b	0.0908	0.0963	0.0816
Final R_1 values (all data)	0.0685	0.0485	0.0518
Final $wR(F_2)$ values (all data)	0.1011	0.1022	0.0885
Goodness of fit on F_2	1.017	1.034	1.025

$^aR_1=\Sigma||Fo|-|Fc||/\Sigma|Fo|$. $^bwR_2= |\Sigma w(|F_o|^2-|F_c|^2)|/\Sigma|w(F_o^2)^2|^{1/2}$

Table. S2 Selected bond lengths [Å] for compound **1**.

N(1)-Cu(1)	2.005(3)	O(7W)-Cu(1)-N(2)	92.22(12)
N(2)-Cu(1)	1.993(3)	O(8W)-Cu(1)-N(2)	162.50(12)
Cu(1)-O(4)	2.247(3)	O(7W)-Cu(1)-N(1)	172.85(12)
O(7W)-Cu(1)	1.951(3)	O(8W)-Cu(1)-N(1)	91.34(12)
O(8W)-Cu(1)	1.959(3)	N(2)-Cu(1)-O(4)	94.84(10)
O(7W)-Cu(1)-O(4)	85.00(12)	N(1)-Cu(1)-O(4)	99.82(10)
O(8W)-Cu(1)-O(4)	102.29(12)		
O(7W)-Cu(1)-O(8W)	92.81(13)		

Table. S3 Selected bond lengths [Å] for compound **2**.

N(1)-Cu(1)	1.9861(18)	N(1)-Cu(1)-O(7W)	91.20(6)
N(2)-Cu(1)	2.0860(19)	O(7W)-Cu(1)-N(2)	125.72(5)
O(7W)-Cu(1)	1.988(3)		

Table. S4 Selected bond lengths [Å] for compound **3**.

N(1)-Cu(1)	2.014(3)	O(7W)-Cu(1)-N(1)	168.80(13)
N(2)-Cu(1)	2.038(3)	O(7W)-Cu(1)-N(2)	94.45(12)
O(7W)-Cu(1)	1.958(3)	N(1)-Cu(1)-O(5)	89.39(11)
O(5)-Cu(1)	2.261(3)	N(2)-Cu(1)-O(5)	82.90(12)
		O(7W)-Cu(1)-O(5)	100.36(13)

Table. S5 Comparison of proton conductivity of compounds with sulfonate groups proton conductors.

Compounds	T (°C)	RH (%)	Proton conductivity (S cm^{-1})	Reference
UiO-66$(SO_3H)_2$	80	90	8.4×10^{-2}	*Angew. Chem. Int. Ed*., 2015, **54**, 5142-5146.
TfOH@MIL-101	60	15	8×10^{-2}	*ACS Appl. Mater.Interfaces*.,2014, **6**, 5161- 5167.
H_2SO_4@ MIL-101	80	20	6×10^{-2}	*J. Am. Chem. Soc*., 2012, **134**, 15640-15643.
$(Me_2NH_2)_3(SO_4)]_2[M_2(ox)_3]$	25	98	4.2×10^{-2}	*Angew. Chem. Int. Ed*., 2014, **53**, 2638-2642.
HOF-GS-11	30	95	1.8×10^{-2}	*Angew. Chem. Int. Ed*., 2016, 55, 10667-10671.
CuH(Hsfpip)Cl(H_2O)	95	97	1.50×10^{-2}	This work
HOF-GS-10	30	95	0.75×10^{-2}	*Angew. Chem. Int. Ed*., 2016, 55, 10667-10671.
$Zr_6O_4(OH)_8L_{4.2}\cdot xH_2O$	65	95	5.62×10^{-3}	*J. Am. Chem. Soc*., 2015, **137**, 11498-11506.
$[Cu(H_2L)(DMF)_4]_n$	95	95	3.46×10^{-3}	*Dalton Trans*., 2015, **44**, 948-954.
H_3PO_4@MIL-101	150	0.13	3×10^{-3}	*J. Am. Chem. Soc*., 2012, **134**, 15640-15643.
CuH_2(Hsfpip)$_2(H_2O)$	95	97	2.58×10^{-3}	This work
Cu-DSOA	85	98	1.9×10^{-3}	*Chem. Commun*., 2013, **49**, 10590-10592.
Cu(Hsfpip)$(H_2O)_2\cdot H_2O$	95	97	1.43×10^{-3}	This work
CB[6]$\cdot 1.2H_2SO_4\cdot 6.4H_2O$	25	98	1.3×10^{-3}	*Angew. Chem. Int. Ed*., 2011, **34**, 7870-7873.
$Cu_4(L)_2(OH)_2(DMF)_2$	95	95	7.4×10^{-4}	*Chem. Commun*., 2015, **51**, 8150-8152.
[Zn(5-sipH)(bpy)]$\cdot$DMF$\cdot 2H_2O$	25	60	3.9×10^{-4}	*Chem. Commun*., 2014, **50**, 1144-1146.
Tb-DSOA	100	98	1.66×10^{-4}	*J. Mater. Chem. A*., 2015, **3**, 641-647.
$[Zn_3$(5-sip)$_2$(5- sipH)(bpy)] $\cdot$ (DMF) $\cdot$2(DMA)	25	60	8.7×10^{-5}	*Chem. Commun*., 2014, **50**, 1144-1146.
$[\{In_2(\mu\text{-}OH)_2(SO_4)_4\}\cdot\{(LH)_4\}\cdot nH_2O]n$	30	98	4.4×10^{-5}	*Inorg. Chem*., 2015, **54**, 5366-5371.
Sr-SBBA	25	98	4.4×10^{-5}	*Chem. Commun*., 2012, **48**, 4998-5000.
TsOH@MIL-101	50	100	3×10^{-5}	*ACS Appl. Mater.Interfaces*., 2014, **6**, 5161-5167.
$[CaL_{0.5}(DMF)_{2.5}]_n$	95	95	1.27×10^{-5}	*Dalton Trans*., 2015, **44**, 948-954.
Ca-SBBA	25	98	8.58×10^{-6}	*Chem. Commun*., 2012, **48**, 4998-5000.
$[CdL_{0.5}(DMF)_2]_n$	95	95	2.49×10^{-7}	*Dalton Trans*., 2015, **44**, 948-954.
$[Zn(H_2O)$(5-sipH)(bpe)$_{0.5}]$ $\cdot$DMF	25	60	3.4×10^{-8}	*Chem. Commun*., 2014, **50**, 1144-1146.

Table. S6 Comparison of proton conductivity among some reported MOFs.

Compounds	T (°C)	RH (%)	Proton conductivity (S cm^{-1})	Reference
UiO-66(SO_3H)$_2$	80	90	8.4×10^{-2}	*Angew. Chem. Int. Ed.*, 2015, **54**, 5142-5146.
Fe-CAT-5	25	98	5×10^{-2}	*J. Am. Chem. Soc.* 2015., **137**, 15394-15397.
(Me_2NH_2)$_3$(SO_4)]$_2$[M_2(ox)$_3$]	25	98	4.2×10^{-2}	*Angew. Chem. Int. Ed.*, 2014, **53**, 2638-2642.
PCMOF-10	60	95	3.55×10^{-2}	*J. Am.Chem. Soc.*, 2015, **137**, 7640-7643.
H+@Ni_2(dobdc)(H_2O)$_2$ (pH = 1.8)	80	98	2.2×10^{-2}	*Angew.Chem. Int. Ed.*, 2014, **53**, 8383-8387.
PCMOF2$^1/_2$	85	90	2.1×10^{-2}	*J. Am. Chem. Soc.*, 2013, **135**, 963-966.
CuH(Hsfpip)Cl(H_2O)	95	97	1.50×10^{-2}	This work
(NH_4)$_2$(H_2adp)[Zn_2(ox)$_3$]·3H_2O	25	98	8×10^{-3}	*J. Am. Chem. Soc.*, 2014, **136**, 7701-7707.
PCMOF-5	62	98	4×10^{-3}	*J. Am. Chem. Soc.*, 2013, **135**, 1193-1196.
[Me_2NH_2][Eu(ox)$_2$(H_2O)]·3H_2O	55	95	2.73×10^{-3}	*J. Mater. Chem. A.*, 2016, 10.1039/C6TA06792A
CuH_2(Hsfpip)$_2$(H_2O)	95	97	2.58×10^{-3}	This work
Cu(Hsfpip)(H_2O)$_2$·H_2O	95	97	1.43×10^{-3}	This work
Fe(ox) • 2H_2O	25	98	1.3×10^{-3}	*J. Am. Chem. Soc.*, 2009, **131**, 3144-3145.
CoCa·nH_2O	25	95	1×10^{-3}	*Chem. Mater.*, 2015, **27**, 8116-8125.
{[Ca(D-Hpmpc)(H_2O)$_2$] • 2$HO_{0.5}$}n	60	97	8.9×10^{-4}	*Chem. Sci.*, 2013, 4, 983-992.
$Ca^{II}Cu^{II}_6$[(*S,S*)-alamox]$_3$(OH)$_2$(H_2O)	80	95	8.6×10^{-4}	*Chem. Mater.*, 2016, 10.1021/acs.chemmater.6b01286.
MFM-500(Ni)	25	98	4.5×10^{-4}	*J. Am. Chem. Soc.*, 2016, **138**, 6352-6355.
In-IA-2D-2	27	98	4.2×10^{-4}	*Chem. Commun.*, 2013, **49**, 6197-6199.
K_2(H_2adp)[Zn_2(ox)$_3$] • 3H_2O	25	98	1.2×10^{-4}	*J. Am. Chem. Soc.*, 2014, **136**, 13166-13169.
{NH(prol)$_3$}[MCr(ox)$_3$]	25	75	1.0×10^{-4}	*J. Am. Chem. Soc.*, 2009, **131**, 13516-13522.
[NMe_3(CH_2CO_2H)][FeCr(ox)$_3$] • nH_2O	25	65	8.0×10^{-5}	*J. Am. Chem. Soc.*, 2012, **134**, 5472-5475.
In-5TIA	28	98	5.35×10^{-5}	*Chem. Commun.*, 2012, **48**, 5464-5466.
(Me_2NH_2)$_2$[$Li_2Zr(C_2O_4)_4$]	17	67	3.9×10^{-5}	*J. Am.Chem. Soc.*, 2015, **137**, 6428-6431.